CWE-8
June 7-11, 2026
London, ON, Canada

CFD of flow characteristics of oscillating multiple flat plates

Nozomi Suzuki [a], Hiroshi Hasebe [b]

[a]*MS Student, Nihon University, Chiyoda-ku, Tokyo, Japan, csno25008@g.nihon-u.ac.jp*
[b]*Associate Professor, Nihon University, Chiyoda-ku, Tokyo, Japan, hasebehiroshi@nihon-u.ac.jp*

SUMMARY

A novel wind power generation system utilizing flutter oscillations of multiple flat plates has been proposed in our research group to efficiently harvest energy within wakes. To clarify the mechanism behind the intense oscillations of these plates, this study conducted a computational fluid dynamics (CFD) analysis of two tandem flat plates. By subjecting the upstream plate to forced vibration, its effect on the downstream plate's oscillation characteristics was investigated. The results revealed that the torsional amplitude of the downstream plate increased sharply as the upstream excitation amplitude rose from 80 degrees to 120 degrees. At an excitation amplitude of 120 degrees, the vortex shed from the upstream plate and the vortex generated at the downstream plate merged. This merged vortex travelled downstream, generating a large negative pressure on the downstream plate's surface. This vortex interaction was identified as the decisive factor causing the sharp amplitude increase.

Keywords: *CFD, flutter, wind power, multiple flat plates, piezoelectric element*

1. INTRODUCTION

Currently, propeller-type wind turbines are widely used for wind power generation. However, the flow formed behind these turbines, known as a wake, is characterized by strong turbulence. This prevents the installation of new turbines downstream without a sufficient separation distance (Crespo and Hernández, 1996). Recently, the adoption of renewable energy has been heavily promoted; however, due to space limitations, solar power generation is more widely used than wind power generation in urban areas. Even in urban environments, there are many places where wind is generated, such as alongside highways and subway platforms, yet a large amount of this energy remains unharvested. Considering this situation, developing a compact, space-saving wind power generation system capable of generating power even within a wake is expected to significantly accelerate wind energy recovery.

From this perspective, our laboratory has been working on the development of a wind power generation system utilizing aeroelastic vibration phenomena within a wake. Nomura et al. (2017) proposed a method to harvest more energy by simultaneously oscillating multiple circular cylinders. However, in their wake galloping system, although the multiple cylinders oscillate violently, the oscillation modes become complex at high wind speeds. This complexity makes it difficult to integrate power generation devices and efficiently recover energy.

In contrast, the present study focuses on the flutter phenomenon. Flutter is a dangerous aerodynamic instability phenomenon in which the oscillation increases divergently with a slight increase in wind speed; however, it possesses enormous kinetic energy capable of causing a bridge collapse (Matsumoto, 2013). In fact, research on wind power generation utilizing the flutter phenomenon is currently underway. Caracoglia (2018) proposed a method to generate power by exploiting the torsional displacement of an isolated wing undergoing large torsional flutter oscillations. Mukogawa et al. (2025) and Wang et al. (2025) are also engaged in similar research on power generation based on wing flutter. However, these studies focus exclusively on the flutter of isolated wings and do not address oscillations within a wake.

Based on the findings from previous wake galloping power generation studies, we hypothesized that energy harvesting could be achieved by replacing circular cylinders with flat plates and utilizing their flutter oscillations. During our preliminary investigation, we confirmed a coupled oscillation phenomenon: placing a second flat plate in the wake of a fluttering upstream plate induced flutter oscillation in the downstream flat plate. Notably, in some cases, the torsional amplitude of the downstream flat plate exceeded that of the upstream flat plate. Because this mechanism enables power generation within a wake, it is highly suitable for application in limited urban spaces. Furthermore, we confirmed that power generation is possible by bringing a flat plate exhibiting flutter-induced torsional oscillation into contact with a fixed piezoelectric element and constructed a wind power generation system based on the flutter oscillation of multiple flat plates. In this mechanism, we developed a system where a square bar attached to the oscillating flat plate contacts a fixed piezoelectric element, successfully generating electric power through the element's deformation (Suzuki and Hasebe, 2025a).

To date, while studies on the oscillation characteristics of the aforementioned parallel circular and square cylinders have been actively conducted, research on the flutter characteristics of flat plates, especially those undergoing large-amplitude oscillations, remains insufficient. Therefore, to understand these characteristics for multiple flat plates, we previously conducted flow visualization experiments and PIV analysis (Suzuki and Hasebe, 2025b). Through the flow visualization experiments, we confirmed that the oscillation behavior of a downstream flat plate within the wake changes significantly depending on the wake conditions generated by the large-amplitude flutter of the upstream plate. Furthermore, the PIV analysis revealed that a strongly pulsating wake flow increased the amplitude of the downstream flat plate, whereas an intermittent wake suppressed it.

However, these previous investigations were limited in scope and involved freely oscillating multiple flat plates; studies with a rigorously controlled wake have not yet been performed. Therefore, in the present study, we utilized computational fluid dynamics (CFD) to subject an upstream flat plate to forced oscillation. By precisely controlling the wake generated by the upstream plate, we investigated its effect on the oscillation characteristics of a downstream flat plate. Through this approach, we aimed to clarify the underlying mechanism of flutter oscillation within a wake.

2. OVERVIEW OF THE POWER GENERATION SYSTEM

The developed power generation system is shown in Figure 1. During the preliminary investigation, we confirmed that multiple flat plates arranged in series along the streamwise direction exhibited strong torsional oscillations even within a wake. Therefore, multiple flat plates were adopted as oscillators for a wind power generation system designed to harvest energy from aerodynamic oscillations. To harvest energy from the flat plate oscillators, piezoelectric elements were utilized. The mechanism features a square bar protruding from the flat plate shown in Figure 1(a). As the flat plate undergoes torsional oscillation, the square bar contacts and deforms the piezoelectric element, thereby generating electric power. The piezoelectric elements were installed externally to avoid obstructing the flow. A conceptual image of the actual installation of our wind-induced vibration power generation system is shown in Figure 1(b). With an assumed span of several tens of centimeters, the system is intended for installation in locations such as subway platforms or building ducts. However, although power generation was successful, we observed instances where the flat plates did not oscillate sufficiently depending on the conditions. Consequently, we initiated a detailed investigation into the oscillation characteristics of multiple flat plates installed within a wake.

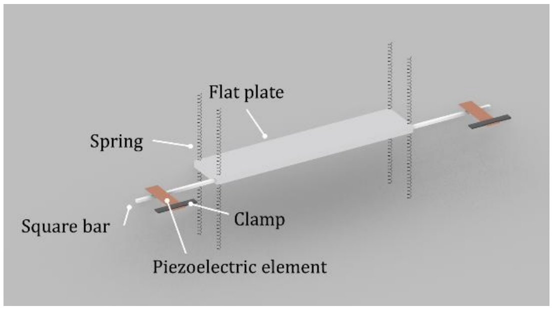

(a) Energy harvesting mechanism using piezoelectric elements

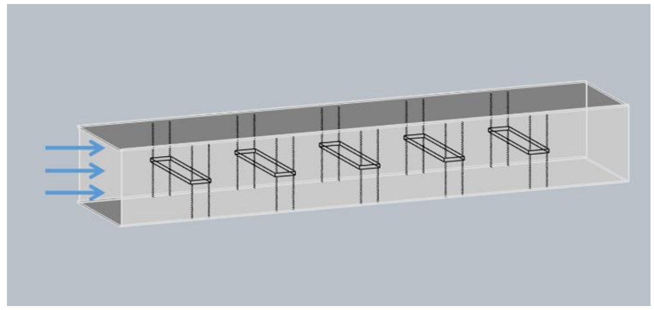

(b) Conceptual image of the installation of the wind-induced vibration power generation system

Figure 1: Overview of the wind-induced vibration power generation system

3. OSCILLATION CHARACTERISTICS OF MULTIPLE FLAT PLATES

First, we measured the torsional amplitude of three flat plates arranged in series within the flow field. Figure 2 shows the experimental conditions, while Table 1 lists the corresponding experimental parameters. Figure 3 shows the relationship between the dimensionless wind speed V_r and the torsional amplitude φ'. The results indicated that while the first and second plates exhibited oscillation amplitudes comparable to those of an isolated flat plate, the amplitude of the third plate was smaller.

Subsequently, flow visualization experiments using smoke were conducted. Figure 4 shows the snapshot of the smoke visualization experiment. From this investigation, it was found that although large vortices were periodically formed at the second plate, these vortices broke down immediately, and no strong pulsation was formed behind it. Consequently, the third plate did not oscillate. In contrast, in the preliminary experiments, all three plates exhibited torsional oscillation and vibrated violently. Therefore, it is evident that the oscillation behavior is highly sensitive to subtle changes in flow conditions.

The findings regarding the oscillation characteristics of multiple flat plates can be summarized by the following three points:

1) While the second plate oscillates with a large amplitude, the third plate's amplitude decreases.

2) However, under certain conditions, all three plates oscillate in a balanced manner, as observed in the preliminary experiments.

3) The oscillation amplitude of the second plate strongly depends on the wake generated by the first plate.

Building on these observations, we sought to identify the specific conditions under which the oscillation amplitude of the plates increases. Therefore, to conduct a systematic parametric study, we decided to perform CFD simulations focusing on a simplified two flat plates configuration.

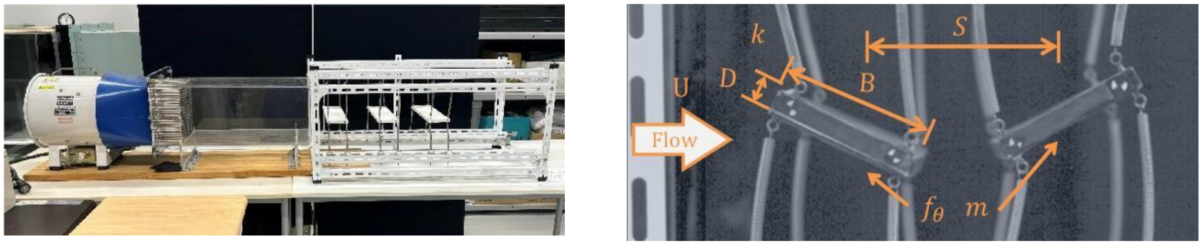

(a) Experimental setup (b) Experimental parameters

Figure 2: Experimental conditions

Table 1: Experimental parameters

Depth D	10 mm
Breadth B	80 mm
Length L	300 mm
Moment of inertia I	$20583\ \mathrm{g \cdot mm^2}$
Wind speed U	$2 \sim 7\ \mathrm{m/s}$
Distance between centers of flat plate S	200 mm

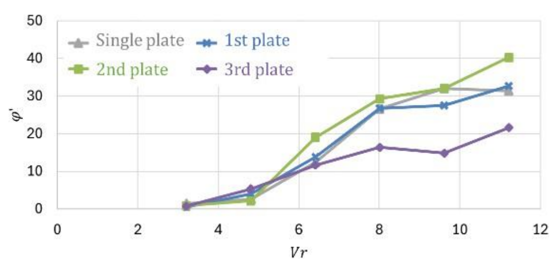

Figure 3: Relationship between the wind speed and the oscillation amplitude of multiple freely oscillating flat plates

Figure 4: Flow visualization around three oscillating flat plates

4. CFD ANALYSIS AND RESULT

4.1. Computational setup and conditions

As described in the previous section, the oscillation behavior of flat plates within a wake was highly complex. To simplify the phenomenon and elucidate the underlying wake oscillation mechanism, we first limited our model to two tandem flat plates and focused on the dynamic response of the downstream flat plate placed in the wake of the upstream flat plate. Because allowing both plates to oscillate freely introduces excessive complexity , we subjected the upstream plate to forced oscillation. By systematically controlling the upstream wake, we can isolate its effect on the downstream plate. Since implementing precise forced oscillation in our physical wind tunnel currently presents experimental challenges, we utilized computational fluid dynamics (CFD) for this investigation.

Figure 5 shows the computational domain and boundary conditions, which generally match the dimensions of the wind tunnel test section. Here, the plate width was $B = 100$ mm, the plate thickness was $D = 10$ mm, and the span length was $L = 10$ mm. However, the size of the flat plate in the spanwise direction was set to $1D$ (D: plate thickness) to reduce computational cost. The influence of the spanwise domain size remains a subject for future study.

At the inlet boundary, a uniform wind speed matching the experimental condition was applied. A slip-wall condition was applied to the side surfaces, a zero-gradient (free outflow) condition at the outlet boundary, and a no-slip condition on the plate surfaces. Table 2 summarizes the analysis parameters, including the oscillation conditions of the flat plates. The excitation amplitude of the upstream flat plate was varied from 20 degrees to 180 degrees (peak-to-peak) in increments of 20 degrees. The excitation frequency was fixed at 11.7 Hz to match the natural frequency of the experimental model.

The simulations were performed using the open-source CFD software OpenFOAM (v2406). The mesh of the entire computational domain is shown in Figure 6. To realize the large-amplitude torsional oscillation of the flat plate, we utilized the Arbitrary Mesh Interface (commonly known as AMI) boundary condition, which dynamically connects solutions between rotating and stationary regions. The mesh around the flat plate was divided into 50 cells in the plate thickness direction, 200 cells in the width direction, and 10 cells in the depth direction. The total number of cells was 1,630,000.

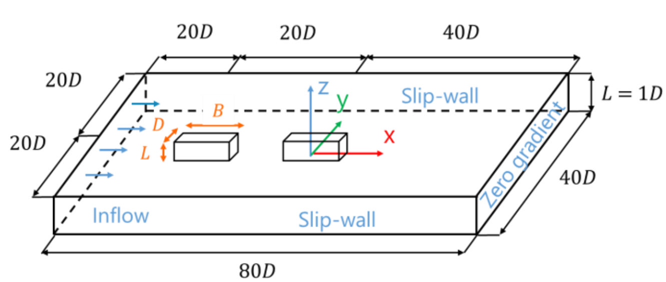

Figure 5: Computational domain and boundary conditions

Table 2: The analysis parameters

Moment of inertia	6.8257×10^{-7} kg/m^4
Damping coefficient	1.96×10^{-6} Nms/rad
Mass	1.27×10^{-3} kg
D.O. F	1-DOF torsional
Plate height D	10 mm
Plate width B	80 mm
Plate spanwise direction L	10 mm
Inflow velocity	6 m/s
Excitation frequency (First plate)	11.7 Hz
Excitation amplitude (First plate)	0 degrees ~180 degrees (20 degrees increments)

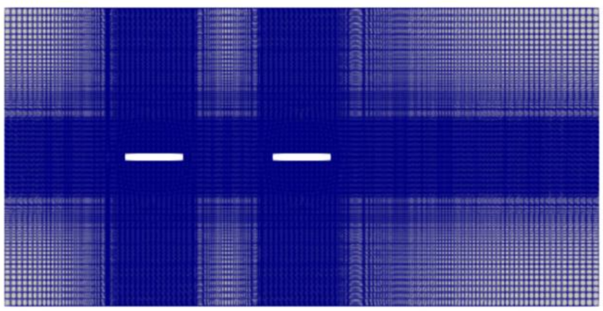
(a) Whole view

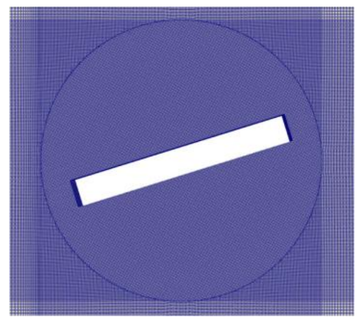
(b) View around a flat plate

Figure 6: Computational mesh

4.2. Analysis result

Figure 7 shows the relationship between the excitation amplitude of the upstream flat plate and the standard deviation of the torsional amplitude (peak-to-peak) of the downstream flat plate. In the range of excitation amplitudes up to 80 degrees, the torsional amplitude of the downstream flat plate increased proportionally. However, as the excitation amplitude was increased to the range of 80 to 120 degrees, the torsional amplitude of the downstream flat plate increased sharply. When the excitation amplitude was further increased, the torsional amplitude of the downstream flat plate conversely decreased. In the following sections, the factors that caused these changes are discussed in detail.

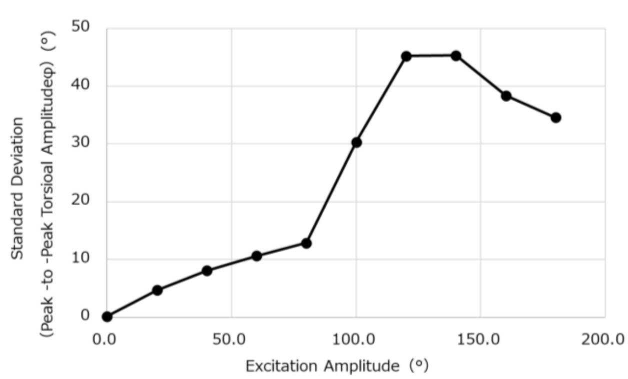

Figure 7: Standard deviation of the peak-to-peak torsional amplitude of the downstream flat plate versus the excitation amplitude of the upstream flat plate

4.3. Case of 80 degrees excitation amplitude

First, we examined the results for an excitation amplitude of 80 degrees for the upstream flat plate, which corresponds to the state just before the sharp increase in the amplitude of the downstream flat plate. Figures 8 and 9 show the pressure distribution and the surface pressure, respectively. It was confirmed that at the moment the vortex shed from the lower surface of the upstream plate passed the lower surface of the downstream plate, the pressure on the lower surface of the downstream plate became increasingly negative, and the magnitude of this negative pressure intensified. Furthermore, the pressure at a position A (-0.02D, -0.04D) relative to the center of the downstream flat plate was extracted to examine its time-series relationship between the amplitude of the downstream flat plate and the pressure (Figure 10). Because a phase difference was observed between the peak of the downward pressure and the oscillation period of the downstream flat plate, we concluded that the vortex shed from the upstream flat plate had little effect on the oscillation of the downstream flat plate at this stage.

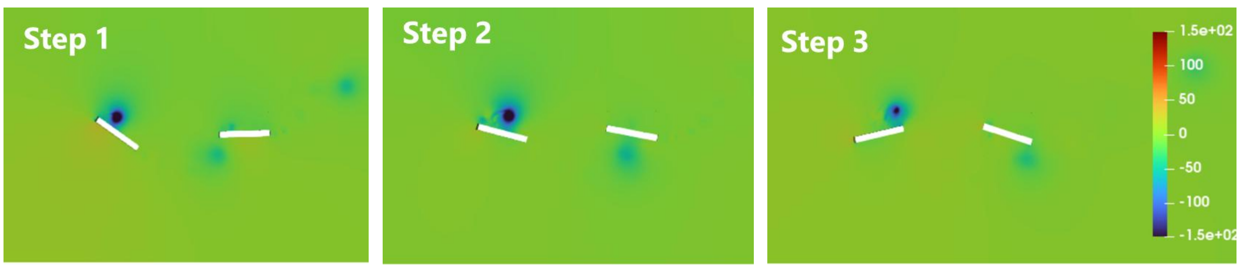

(a) Vortex shedding from the upstream flat plate (b) Convection of the vortex (c) Passage of the vortex

Figure 8: Pressure distribution during the downstream convection of the vortex shed from the upstream flat plate (Excitation amplitude of 80 degrees)

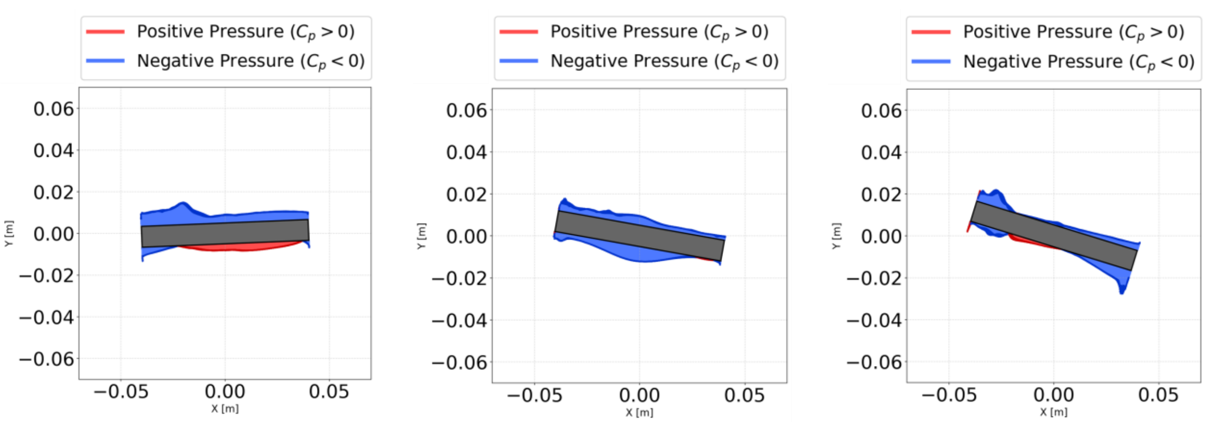

(a) Vortex shedding from the upstream flat plate (b) Convection of the vortex (c) Passage of the vortex

Figure 9: Surface pressure distribution on the downstream flat plate during the downstream convection of the

vortex shed from the upstream flat plate (Excitation amplitude of 80 degrees)

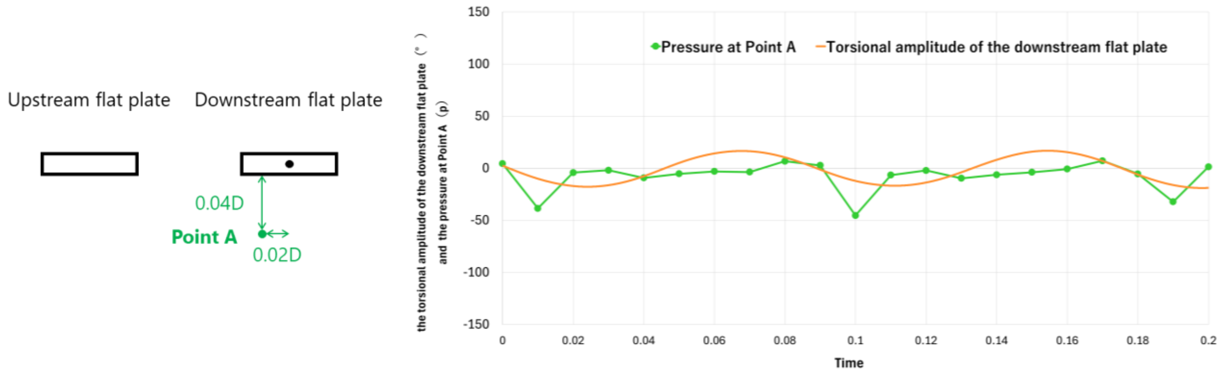

Figure 10: Time histories of the pressure at Point A and the torsional amplitude of the downstream flat plate (Excitation amplitude of 80 degrees)

4.4. Case of 120 degrees excitation amplitude

Next, we describe the results for an excitation amplitude of 120 degrees for the upstream flat plate, which corresponds to the stage where the amplitude of the downstream flat plate sharply increases. Figures 11 and 12 show the pressure distribution and the downstream plate's surface pressure, respectively. Similarly, Figure 13 shows the corresponding time-series data for the 120 degrees excitation case.

In Step 1, the vortex shed from the upstream flat plate was observed passing beneath the lower surface of the downstream flat plate. In the subsequent Step 2, two distinct vortices were observed: the vortex generated by the downstream flat plate and the vortex convecting from upstream. At this instant, the surface pressure distribution shows that a substantial negative pressure was induced on the lower surface of the downstream plate. Subsequently, in Step 3, the vortex from upstream and the vortex generated at the downstream plate merged. As this merged vortex convected further downstream, the negative pressure on the lower surface decreased compared to the level observed in Step 2.

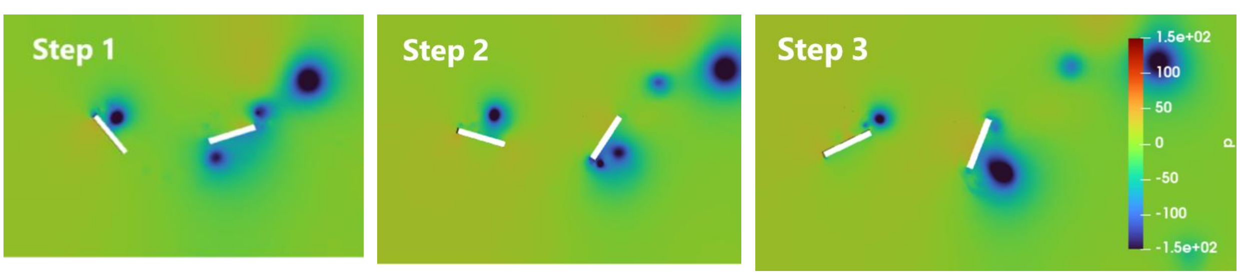

(a) Vortex shedding from the upstream flat plate

(b) Two Types of Vortexes

(c) Vortex Coupling

Figure 11: Pressure distribution during the downstream convection of the vortex shed from the upstream flat plate (Excitation amplitude of 120 degrees)

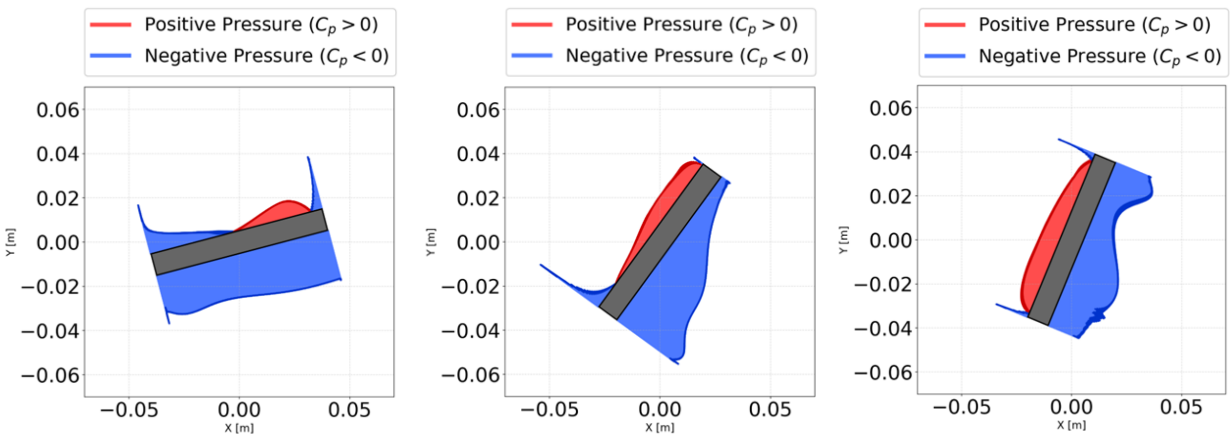

(a) Vortex shedding from the upstream flat plate

(b) Two Types of Vortexes

(c) Vortex Coupling

Figure 12: Surface pressure distribution on the downstream flat plate during the downstream convection of the vortex shed from the upstream flat plate (Excitation amplitude of 120 degrees)

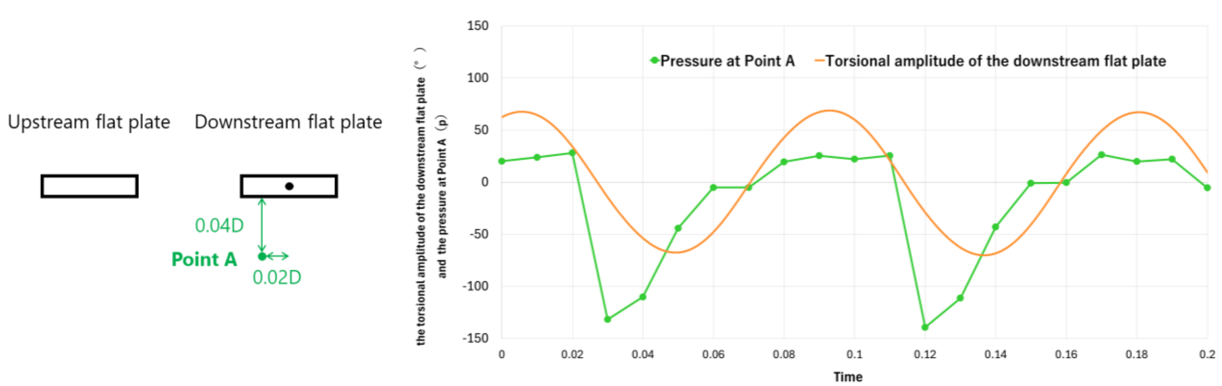

Figure 13: Time histories of the pressure at Point A and the torsional amplitude of the downstream flat plate (Excitation amplitude of 120 degrees)

5. CONCLUSIONS

In this study, to develop a novel wind power generation system using flutter oscillations of multiple flat plates that can efficiently harvest energy even within a wake, CFD analysis was conducted using two tandem flat plates. By subjecting the upstream plate to forced vibration and varying its excitation amplitude, the effects on the oscillation characteristics of the downstream plate were investigated. The following findings were obtained:

1) Up to an excitation amplitude of 80 degrees for the upstream flat plate, the torsional amplitude of the downstream plate increased proportionally to the excitation amplitude. However, the amplitude of the downstream plate exhibited a sharp surge as the excitation amplitude rose from 80 to 120 degrees, and subsequently tended to decrease when the excitation amplitude was increased further.

2) At an excitation amplitude of 80 degrees, which was the stage before the sharp increase in the downstream amplitude, a phase difference was observed between the peak negative pressure caused by the vortex convecting from upstream and the oscillation cycle of the downstream plate. This confirmed that the vortex from upstream had a relatively small effect on the oscillation of the downstream plate at this stage.

3) Conversely, at an excitation amplitude of 120 degrees, where the downstream amplitude increased sharply, the vortex shed from the upstream plate and the vortex generated at the downstream plate were observed to merge. As the merged vortex convected further downstream, a substantial negative pressure was generated on the lower surface of the plate. This result suggests that the interaction and merging of these two types of vortices act as the decisive factor causing the sharp increase in the amplitude of the downstream flat plate.

In future work, forced vibration experiments incorporating flow visualization will be conducted to experimentally verify whether the vortex merging phenomenon identified by the present analysis occurs in actual fluid flows.

ACKNOWLEDGEMENTS
This work was supported by The Maeda Engineering Foundation.

REFERENCES

Caracoglia, L., 2018. Modeling the coupled electro-mechanical response of a torsional-flutter-based wind harvester with a focus on energy efficiency examination, Journal of Wind Engineering and Industrial Aerodynamics 174, 437-450.

Crespo, A., Hernández, J., 1996. Turbulence characteristics in wind-turbine wakes, Journal of Wind Engineering and Industrial Aerodynamics 61, 71-85.

Matsumoto, M., 2013. Flutter and its application - Flutter mode and ship navigation, Journal of Wind Engineering and Industrial Aerodynamics 122, 10-20.

Mukogawa, T., Shimura, K., Dong, S., Fujita, K., Nagai, H., Kameyama, M., Shi, Y., Jia, Y., Souits, C., Kurita, H., Narita, F., Hara, Y., Makihara, K. and Otsuka, K., 2025. Piezoelectric flutter energy harvesting: Absolute nodal coordinate formulation model and wind tunnel experiment, Mechanics Research Communications, 143, 104351.

Nomura, T., Saegusa, N. and Hasebe, H., 2017. Vibration of Multiple Circular Cylinders in Tandem Alignment, Proceedings of the First International Symposium on Flutter and its Application –ISFA2016-, 385-392.

Suzuki, N. and Hasebe, H., 2025a. Vibration characteristics of multiple flat plates based on flow visualization, Proceedings of the 9th European African Conference on Wind Engineering -EACWE9-.

Suzuki, N. and Hasebe, H., 2025b. PIV analysis of flow characteristics of oscillating multiple flat plates, Proceedings of the 10th Asia-Pacific Conference on Wind Engineering -APCWE10-.

Wang, K., Xia, W., Zhong, X., Tang, K., Liao, Z. and Hu, S., 2025. Enhancing energy harvesting efficiency by utilizing twisting kinematics in flutter-driven wind energy harvester, Journal of Physics D: Applied Physics, 58, 425502.